ARMA 19–2086

Modeling the Impact of Interfaces in a Layered Rock on Fracture Propagation and Resulting Height

Chad C. Hammerquist
FracGeo, The Woodlands, TX, USA
John A. Nairn
Oregon State University, Corvallis, OR, USA
Yamina Aimene and Ahmed Ouenes
FracGeo, The Woodlands, TX, USA

This paper was prepared for presentation at the 53rd US Rock Mechanics/Geomechanics Symposium held in New York, NY, USA, 23–26 June 2019. This paper was selected for presentation at the symposium by an ARMA Technical Program Committee based on a technical and critical review of the paper by a minimum of two technical reviewers. The material, as presented, does not necessarily reflect any position of ARMA, its officers, or members. Electronic reproduction, distribution, or storage of any part of this paper for commercial purposes without the written consent of ARMA is prohibited. Permission to reproduce in print is restricted to an abstract of not more than 200 words; illustrations may not be copied. The abstract must contain conspicuous acknowledgement of where and by whom the paper was presented.

ABSTRACT

A new method is introduced for modeling fluid-driven fracture propagation by coupling explicit fracture propagation in MPM with a lower-dimensional diffusion flow model along the fracture. This new method was tested with multiple numerical experiments of fracture propagation in layered materials with interfaces. The model was able to reproduce pertinent laboratory and field observations, like fracture arresting, fracture curving, and the potential to reduce fracture growth in stacked layered media.

INTRODUCTION

Modeling hydraulic fracturing is important and necessary to understand the process in order to optimize production and maximize the economics of unconventional reservoirs. A major component of this process is obviously fluid driven fracture propagation which is a complex multiscale physics problem, that is modeled in this paper using the Material Point Method (MPM). The Material Point Method (MPM) has emerged as a valuable tool for modeling these reservoirs because it allows modeling arbitrarily complex material models by using the anisotropic damage mechanics models (Nairn, Hammerquist and Aimene, 2017), can handle multiple distinct materials (Nairn 2007), accurately models discontinuities such as material interfaces (Nairn, 2007, Aimene et al., 2018) and fractures including dynamic fracture propagation (Nairn, 2003; Guo and Nairn, 2004 and 2006), can include fully coupled poroelasticity (Khodabakhshnejad et al, 2017) as well as viscoelasticity (Peterson et al. 2018) and can natively handle solid-fluid interactions (Hammerquist, Nairn 2018). MPM is a hybrid method that uses a two different discretizations to approximate and solve the conservation of momentum and conservation of mass equations. The material domain is approximated with a particle basis, or Lagrangian material points, which move around and store mass, velocity, deformation, stress and possibly other history dependent data. The second basis is a background grid which is fixed and rectangular to allow for easy calculation of spatial gradients. The grid is overwritten at every time step and is considered to be an "update reference" and so the nonlinear

convective terms from Eulerian formulations are not needed (Sadeghirad et al., 2011). At each time step, particle information is interpolated to the grid, which is used as a tool space to solve the equations of motions. This updated information is interpolated back to the particles. This use of both particles and grid combines advantages of both mesh-based methods and particle-based methods.

In a previous attempt to model fluid driven fracture propagation with MPM, the fluid inside the fracture was handled directly as a fully modeled material that interacted with the fracture surfaces with contact (Raymond et al., 2015). While this approach is useful to highlight the observation at the fracture scale, the resolution needed to accurately resolve the fluid flow requires a specific treatment to accommodate large reservoir simulations. Here we introduce another technique to model this problem, lower dimensional fluid diffusion along the manifold provided by the explicit fracture in MPM.

METHODS

A method for explicitly modeling fractures in MPM was developed and named CRAMP (Nairn 2003). In a 2D CRAMP simulation, a fracture is represented by a series of fracture points connected with line segments. An example of a CRAMP fracture is shown below in Figure 1. This assembly of points and line segments delineates the fracture discontinuity and translates with the background material. This spatial discontinuity is created by changing the interpolation between material points and grid nodes. Grid nodes near the fracture have multiple material fields. Information from the material points is mapped to different material fields on a particular node depending on which side of the fracture the node and the particle are on. These multiple material fields allow for correct treatment of fracture discontinuity including handling contact of the fracture surfaces. This setup also allows for accurate tracking of the fracture surfaces which are needed for calculating certain properties including J-integral and stress intensity factors (Guo and Nairn 2006). Fracture propagation is achieved by inserting a new fracture point in front of the fracture tip. This formulation of fractures also allows traction laws, cohesive laws, or pressure to be added to the fracture surfaces. These forces are calculated on the fracture point from the corresponding traction law from the area of the fracture segment and then interpolated to the grid. For 3D CRAMP simulations, the fracture surfaces are represented by fracture particles connected with triangle elements (Guo and Nairn 2017), an example of a 3D CRAMP fracture is shown in Figure 1.

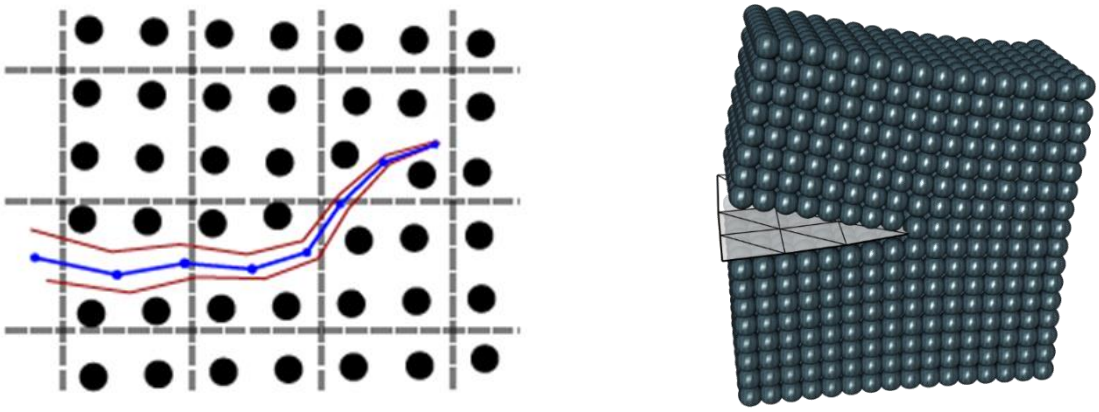

Figure 1 (Left) An explicit 2D CRAMP fracture in an MPM simulation. The fracture plane is shown in blue with the fracture particles shown as the blue dots and the fracture surfaces as red lines. Black dots are material points and dashed lines are the background grid. (Right) An explicit CRAMP fracture in a 3D MPM simulation.

A pressure law can be applied to the fracture surfaces to model the effect of a hydraulically driven fracture in a MPM simulation with a CRAMP fracture. But this pressure should be provided by the physics of the problem. To accomplish that, we added a nested simulation to model the fluid flow inside the fracture. The assembly of fracture particles and segments form a manifold on which to run this nested simulation. In a 2D MPM simulation with an explicit fracture, the fracture forms a 1D manifold embedded in the 2D simulation space. In a 3D MPM simulation, the fracture surface would form a 2D manifold.

To model the flow along the fracture, the height-averaged laminar flow in a channel can be calculated as

$$\mathrm{v} = -\frac{w^2}{12\mu}\frac{dP}{dx} \tag{1}$$

Where v is velocity, w is the height of the channel, μ is fluid viscosity and P is pressure. A linear constitutive law for the fluid is defined as:

$$\frac{\partial P}{\partial t} = M\frac{\partial \mathrm{v}}{\partial x} \tag{2}$$

Where M is the bulk modulus of the fluid. Combining equations (1), (2) gives the familiar diffusion equation

$$\frac{\partial P}{\partial t} = \frac{M}{\mu}\frac{\partial}{\partial x}\left(k\frac{\partial P}{\partial x}\right) \tag{3}$$

Where k is the permeability of the fracture defined from equation (1):

$$k = \frac{w^2}{12} \tag{4}$$

In our simulations, equation (4) is solved using a finite difference method on the discretiziation provided by the crack points. The time integration was solved with the trapezoid method because it is second order accurate and unconditionaly stable. At each time step of the MPM simulation, the fracture

opening is updated in the 1D diffusion solver, then the updated pressure from this solver is applied to fracture surfaces.

An example of this coupled fracture simulation is shown below in Figure 2. An infinite elastic half-domain is approximated with an 80m x 80m region with applied surface tractions and a symmetery condition at the bottom. A pressure condition is set at the inlet of the fracture. A snapshot in time of the pressure distribution along the fracture is shown in Figure 2. The fracture width and resulting permeablility along the fracture are also shown.

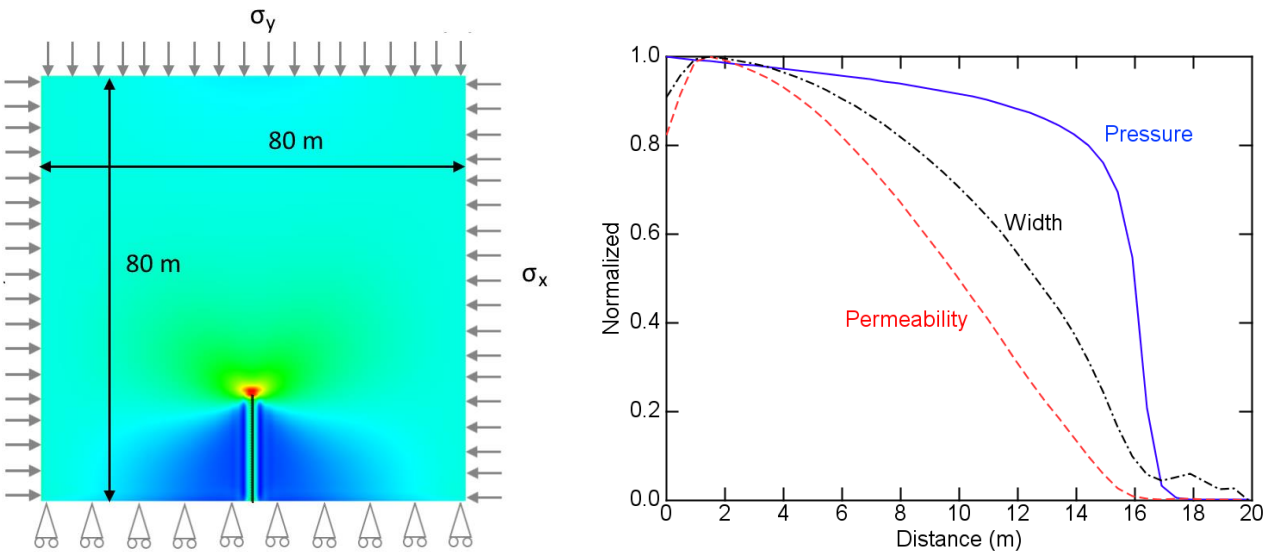

Figure 2 (Left) An example of an MPM simulation with a pressurized explicit fracture. Color shows stress in horizontal direction. (Right) A snapshot of the normalized pressure profile along the fracture as well as the fracture opening and corresponding permeability.

NUMERICAL EXPERIMENTS AND RESULTS

To demonstrate the usefulness and capabilities of this formulation of MPM and diffusion flow, six numerical experiments are carried out. In all the numerical experiments, the simulation domain and boundary conditions are the same as given in Figure 2. The MPM resolution was 1m per cell. For all but the last experiment, 3 MPa of background stress was applied in vertical direction and 2 MPa stress in the horizontal direction. The initial fracture height was 5 m. The fluid properties were the same for all the simulations with $M = 1$ GPa and $\mu = 0.1$ Pa $\cdot s$. The fluid pressure at the inlet was ramped up at a rate of 0.35 MPa/s. The fracture propagation criteria was based on the J-integral criteria.

To make these simulations more applicable to real world situations, the effect of interfaces on fracture height is also considered. Three different types of interfaces were used, a friction interface, a weak interface and and a soft interface. In the friction interface, the materials at the interfaces interact with each

other by contact and Coulumb friction. In the weak interface, the interface acts as a perfect interface as long as the forces at a given point meet the criteria:

$$\left(\frac{S}{S_c}\right)^2 + \left(\frac{N}{N_c}\right)^2 < 1 \tag{5}$$

where S and N are the stresses at the interface in the shear and normal direction respectively. Once the stresses exceed the critial stresses as given in Equation 5, the interface fails and no longer transfers load at this point. The soft interface does not fail, but has a lower stiffness then the surrounding material. The tractions on these interfaces are calculated from the seperation at the interface:

$$T_n = D_n u_n \text{ and } T_t = D_t u_t \tag{6}$$

Where the subscript denotes the normal or tangential component, D is the stiffness coefficient of the interface and u is the relative interface displacement. More details of implementation of these interfaces can be found in (Nairn 2007,2013).

Experiment 1

In this first set of experiments the background material had a stiffness of E=10 GPa with the Poisson's ratio $\nu = 0.2$ and $K_{Ic} = 1.45MPa\sqrt{m}$. An interface perpendicular to the fracture was included in the simulation domain. The location of the interface relative to the initial fracture is shown below in Figure 3. The fracture height vs pressure for simulations with the different types of interfaces are shown below in Figure 3. For this example, the friction interface had a friction coefficient of 0.4, the weak interface had strengths $S_c = 0.5MPa$ and $N_c = 0.5MPa$ and the soft interface had stiffnesses $D_n = 0.5MPa/m$ and $D_t = 0.5MPa/m$. Even at the relatively low friction coefficient, the frictional interface had a limited impact on the fracture height. But both the weak and soft interfaces arrested the fracture propagation until the pressure increased enough to continue driving the propagation. With the weak interface, the fracture behaved as in the bulk material without interface, then sheared at low pressure when reaching the interface, while with soft inteface, the interface shearing appeared at the biggining of the pressurization.After fracture arresting, both interfaces showed a plateau behavior for similar pressure difference.

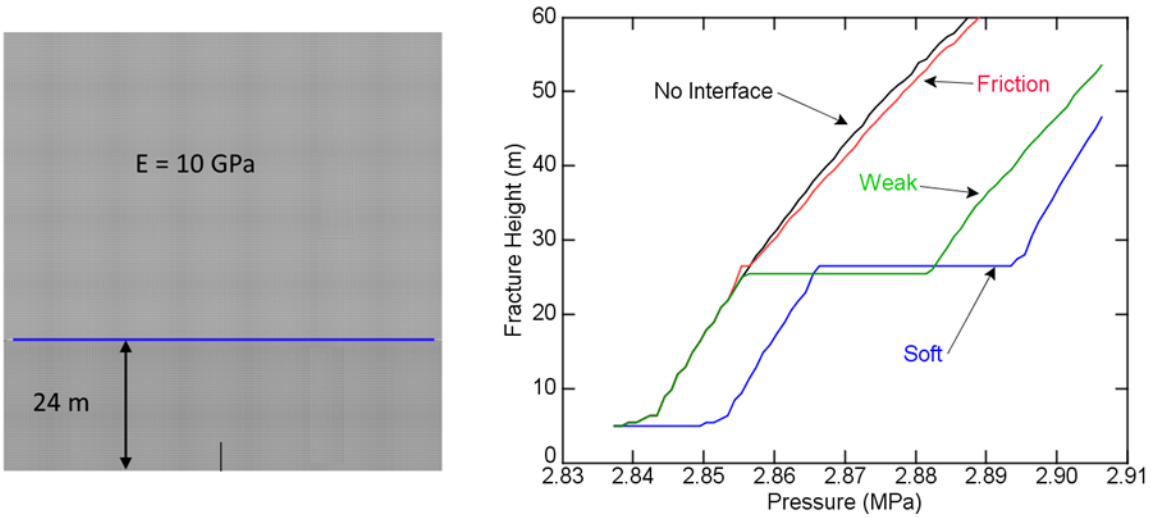

Figure 3 (Left) Interface position (shown in blue) and simulation domain for first numerical example. (Right) Fracture lengths vs inlet pressure for different interface types.

Experiment 2

The simulation setup for Experiment 2 is similar to Experiment 1 except that the interface separates two distinct materials. The initial lay out of this experiment is shown below in Figure 4. The fracture started in a stiffer layer with Young's modulus E=10 GPa, Poisson's ratio $\nu = 0.2$ and $K_{Ic} = 1.45MPa\sqrt{m}$ and eventually propagated into a soft layer with E=5 GPa with the Poisson's ratio $\nu = 0.2$ and $K_{Ic} = 1.25MPa\sqrt{m}$. For this example, the friction interface had a friction coefficient of 0.6, the weak interface had strengths $S_c = 0.5MPa$ and $N_c = 0.5MPa$ and the soft interface had stiffnesses $D_n = 0.5MPa/m$ and $D_t = 0.5MPa/m$. The fracture heights vs inlet pressure for the different cases are shown below in Figure 4. In this example, the fracture propagation is affected by the presence of the softer material. The weak and softer interfaces showed same trend as a perfect interface. The frictional interface, has a similar overall behavior but with a propagation starting earlier at low pressure. However, the presence of softer layer reduced the plateau behavior but delayed substantially the propagation initaition compared to previous sample with same material.

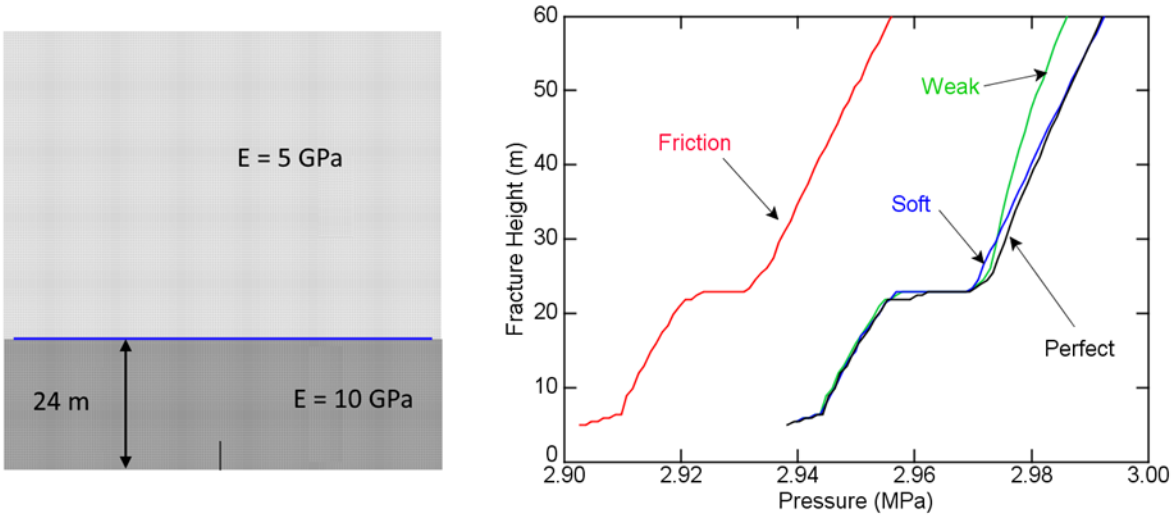

Figure 4 (Left) Interface (shown in blue) and materials position and simulation domain for second numerical example. (Right) Fracture lengths vs inlet pressure for different interface types.

Experiment 3

In this set of numerical experiments, a second interface was added to the simulation setup from Experiment 1. The layout of the interfaces is shown below in Figure 5. Two different combinations of interface types are considered. In the first simulation the first interface is a weak interface and the second interface is a soft interface. In the second simulation this order is switched. The interface parameters are the same as in Experiment 2. The fracture heights are shown below in Figure 5. The fracture height is drastically impacted by the presence of two interfaces compared to the perfect interface. Samples with interfaces arrested the fracture propagation, but the weak then soft interfaces case showed a longer first plateau behavior as well and a second fracture arrest at the second interface, thus requiring higher pressure to propagate the fracture further. These cases highlight the potential of interfaces density in the reservoirs in reducing the propagation potential of the hydraulic fracture, as its energy is used to shear or delaminate the interfaces.

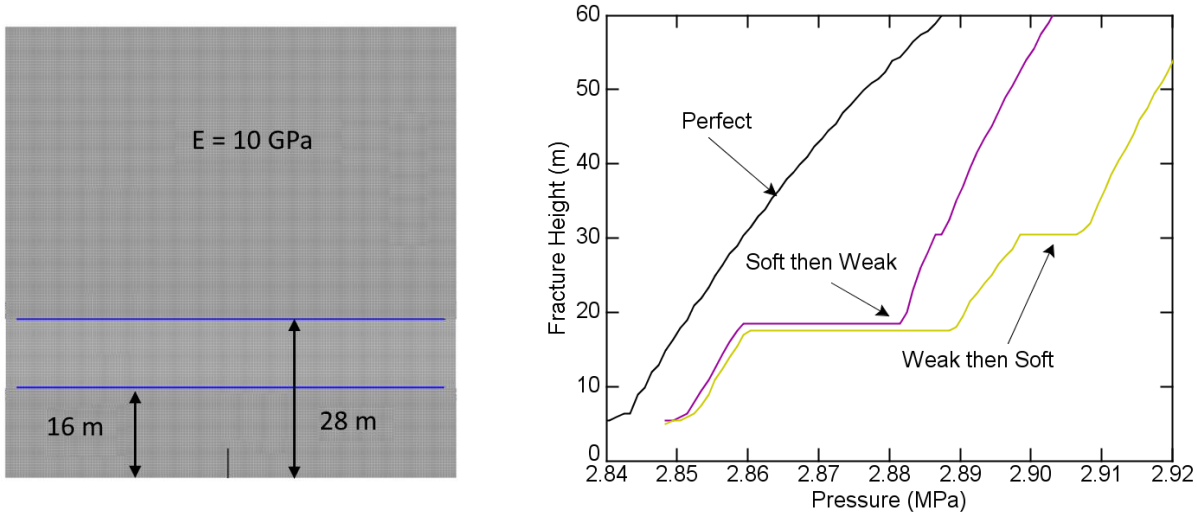

Figure 5 Interface (shown in blue) and materials position and simulation domain for third numerical example. (Left) Fracture lengths vs inlet pressure for different interface types.

Experiment 4

In this set of numerical experiments, the simulation domain is the same as in Experiment 3, except there is a softer material between the interfaces. The simulation layout is shown below in Figure 6. Also, both of the interfaces properties are the same and the material properties are the same as in Experiment 3. The fracture heights are shown below in Figure 6. The frictional interface between the soft and stiff materials has a significant effect on propagation. Unlike in experiment 2, the fracture was arrested at the first interface only, and no plateau behavior was observed at the second interface as illustrated in figure 7, probably because of the used fracture toughnesses.

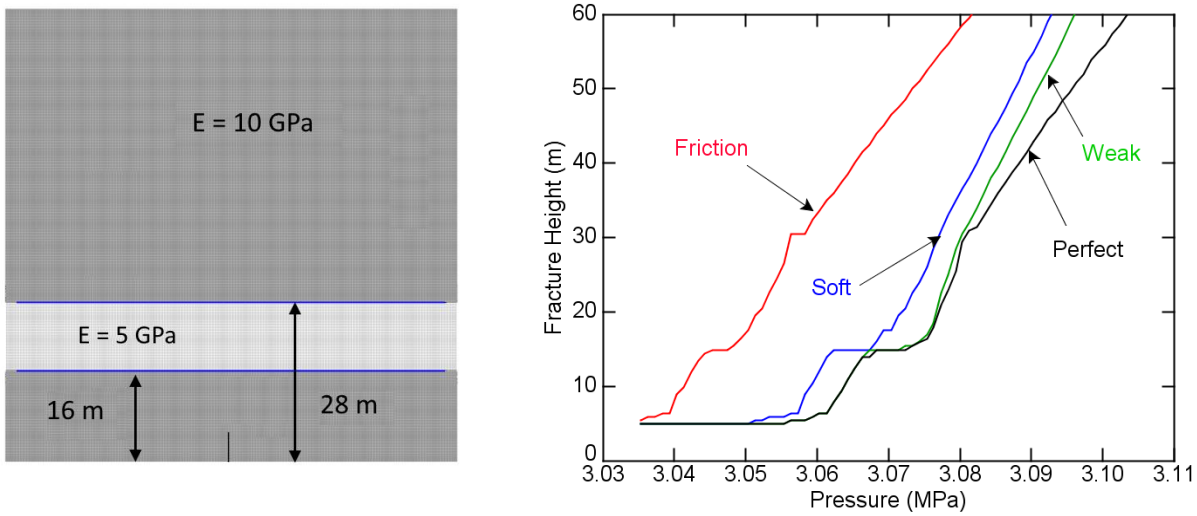

Figure 6 Interface and materials position and simulation domain for fourth numerical example. (Right) Fracture lengths vs inlet pressure for different interface types.

Figure 7 shows the fracture opening at several times, calculated from the fracture points in the MPM simulation in the case of the weak interface. For comparison, the fracture opening of the simulation with a perfect interface is also shown as a dotted line at one time. According to the estimated fracture profile,

perfect interfaces generated continuous fracture propagation while, weak interface showed a fracture arrest at the first interface only.

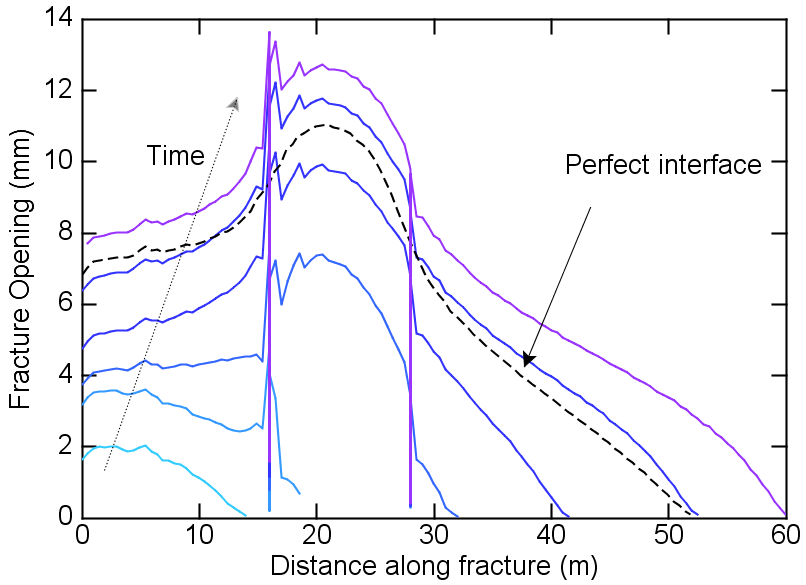

Figure 7 Fracture profiles for the fourth numerical example for the simulation with the weak interface. The crack profile is compared to the simulation with perfect interfaces (dotted).

Experiment 5

In this set of numerical experiments, the simulation domains are the same as the previous and the material and interfaces are the same as in Experiment 2. However, interfaces between materials is parallel to the direction of the initial fracture propagation. The initial layouts for these numerical experiments are shown below as insets in Figure 8. In these experiments, the fracture starts in the soft material and deviates away from the stiff material regardless of the interface types. Thus, the stiff material played a role of fracture propagation barrier. These fracture paths are shown below in Figure 8.

Experiment 6

The layout of this set up of simulations is similar to Experiment 5, except here the fracture starts in the stiff material. Also, the background stress state is different: the vertical applied stress is 1 MPa and the horizontal stress is 2 MPa. As is expected the fractures turn into the soft layer and follow the direction of maximum stress. In both last experiments, only the soft interface had a significant impact on the fracture path.

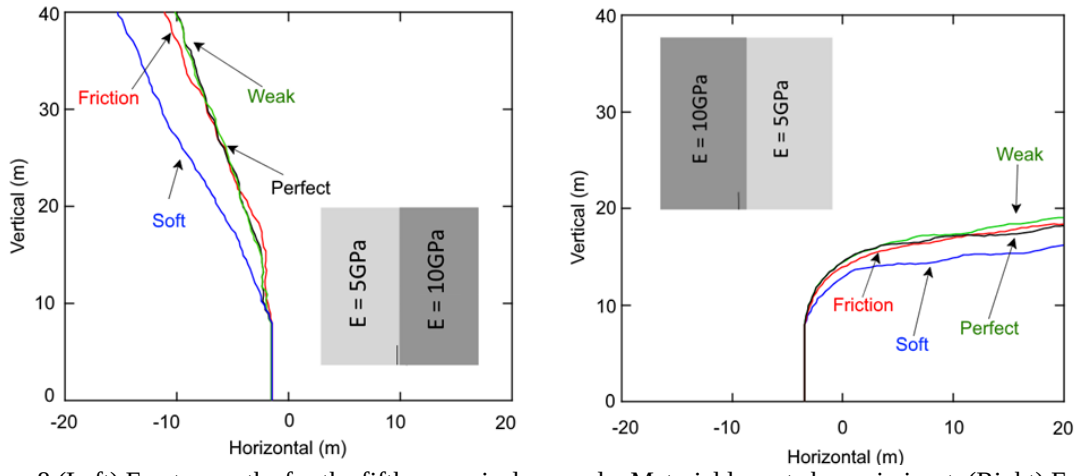

Figure 8 (Left) Fracture paths for the fifth numerical example. Material layout shown in inset. (Right) Fracture paths for sixth numerical example.

CONCLUSIONS

Coupling explicit fracture propagation in MPM with a diffusion flow model is a promising method for modeling fluid driven fracture propagation and allows for more physics to be included. The model was able to reproduce pertinent laboratory and field observations, like fracture arresting, fracture curving, and the potential to reduce fracture growth in stacked layered media.

REFERENCES

Aimene, Y., Hammerquist, C.C, Nairn, J., and Ouenes, A., 2018, 3D Anisotropic Damage Mechanics for Modeling Interaction Between Hydraulic and Natural Fracture Planes in a Layered Rock– Application to Eagle Ford and Wolfcamp. Paper no 2902985 presented at Unconventional Resources Technology Conference (URTeC), Houston, TX, USA.

Guo, Y. and Nairn, J.A., 2004. Calculation of J-integral and stress intensity factors using the material point method. Computer Modeling in Engineering and Sciences, 6, pp.295-308.

Guo, Y.J. and Nairn, J.A., 2017. Simulation of dynamic 3D fracture propagation within the material point method. cmes-computer modeling in engineering & sciences, 113(4), pp.389-410.

Hammerquist, C.C., Nairn, J.A., 2018. Numerical simulation of pressure-driven adhesive penetration into realistic wood structures Wood Science and Technology 52: 1271. https://doi.org/10.1007/s00226-018-1032-z

Khodabakhshnejad, A., Aimene, Y., Mistry, N., Bachir, A. and Ouenes, A., 2017. A Fast Method to Forecast Shale Pressure Depletion and Well Performance Using Geomechanical Constraints-Application to Poro-Elasticity Modeling to Predict Mid and Far Field Frac Hits at an Eagle Ford and Wolfcamp Well. In SPE Eastern Regional Meeting. Society of Petroleum Engineers. doi:10.2118/187535-MS

Nairn, J.A., 2003. Material point method calculations with explicit fractures. Computer Modeling in Engineering nd Sciences, 4(6), pp.649-664.

Nairn, J.A., Hammerquist, C.C. and Aimene, Y.E., 2017. Numerical implementation of anisotropic damage mechanics. International Journal for Numerical Methods in Engineering, 112(12), pp.1848-1868.

Nairn, J.A., 2007. Numerical implementation of imperfect interfaces. Computational Materials Science, 40(4), pp.525-536.

Nairn, J. A. (2013). Modeling imperfect interfaces in the material point method using multimaterial methods. Comput. Model. Eng. Sci, 92, 271-299.

Peterson, N., Ouenes, A., Ng, M., Hughes, R., Hlidek, B., Aimene, Y.,Li, X., 2018. Case study of time-based stress shadow influences on new well fracture propagation patterns in the Montney. Society of Petroleum Engineers. doi:10.2118/189813-MS

Raymond, S., Aimene, Y., Nairn, J. and Ouenes, A., 2015, Coupled fluid-solid geomechanical modeling of multiple hydraulic fractures interacting with natural fractures and the resulting proppant distribution. In SPE/CSUR Unconventional Resources Conference. Society of Petroleum Engineers. doi:10.2118/175972-MS

Sadeghirad, A., Rebecca M. Brannon, and J. Burghardt., A convected particle domain interpolation technique to extend applicability of the material point method for problems involving massive deformations. International Journal for Numerical Methods in Engineering 86.12 (2011): 1435-1456.